Minimizing the Formation of Polynuclear Pd(II) Hydroxo Complex Clusters in Biomineralization of Barley Stripe Mosaic Virus

Che-Yu Chou [a], Catherine Ma [a], Josephine Lesley Liebrata [a], Justin Blake White [a], L. Sue Loesch-Fries [b], Michael T. Harris [a, *]

AUTHOR ADDRESSES

[a] 480 Stadium Mall Drive, School of Chemical Engineering, Purdue University, West Lafayette, IN 47907, United States

[b] 915 West State Street, Department of Botany and Plant Pathology, Purdue University, West Lafayette, IN 47907, United States

* Corresponding author: mtharris@purdue.edu

KEYWORDS

Biotemplate, Barley stripe mosaic virus (BSMV), Hydrolysis

Abstract

The Barley stripe mosaic virus (BSMV) has been successfully adopted to synthesize metal-organic nanorods of high quality. The biomineralization of palladium takes place without the presence of a reducing agent. However, $PdCl_4^{2-}$, the precursor used in mineralization, forms hydrolyzed chloropalladate species in aqueous media. More highly hydrolyzed chloropalladate species can cause the formation of clusters that can affect the coating quality of the palladium metal on the surface of the biotemplate. The aim of this research is to minimize the formation of hydrolyzed chloropalladate clusters. The stability constants of hydrolyzed chloropalladate species were studied and utilized to calculate the distribution of hydrolyzed chloropalladate species as a function of initial Na_2PdCl_4 concentration. The calculations show that high initial concentration of Na_2PdCl_4 favors the stability of the solution. Besides, dilute hydrochloric acid solutions were used in the preparation of the tetrachloropalladate precursor stock solution. The metal precursor stock solution was stable for up to 30 days. Preliminary study of the hydrolysis reaction was evaluated by dynamic light scattering. Additionally, the effect of preheating on the morphology of Pd-BSMV nanorods was compared and evaluated. Finally, the Pd-BSMV nanorods prepared from the HCl-added Na_2PdCl_4 stock solution contained minimized irregular-shaped palladium particles.

Introduction

Biotemplating has been developed as an alternative nanomaterial synthesis method because it has been reported to generate uniform and monodisperse structures[1]. Moreover, materials produced from this route tend to be green and economical[2]. Various biomolecules, such as DNA[3], cellulose[4], bacteria[5], viruses[6], have been employed to produce materials of high-quality. These materials are promising in applications such assensing[4], catalysis[5], imaging[7], and electronics[8]. Plant viruses are particularly attractive in material synthesis as they possess a wide range of sizes and shapes and exhibit diverse chemical functionalities[9]. For example, the tobacco mosaic virus (TMV) has been adopted as the biotemplate for the mineralization of metallic nanoparticles such as Pd[10], Pt[11], Ag[10], and Au[12].

The mineralization process is usually achieved by introducing metal ion precursors to the templates in the presence of a reducing agent[10, 13], which allows the precursors to be reduced and deposited onto the surface of the template. Previously, Lim et al. demonstrated that the mineralization of palladium nanoparticles can be obtained without adding external reducing agents[1]. Furthermore, the morphology of palladium coatings without a reducing agent was found to be more uniform and controllable than that with the addition of the reducing agent. It is noteworthy that the amount of added precursor is highly associated with the quality of coating. With the presence of a reducing agent, both adsorbed and free precursors would be reduced, leading to the formation of irregular-shaped nanoclusters on the surface of biotemplate. On the other hand, when the amount of added precursor was regulated and without the presence of a reducing agent, the precursors were able to adsorb onto the surfaces of the template and then be reduced by the surface functionalities at an elevated temperature, resulting in the formation of uniform coatings. This mineralization process was called hydrothermal synthesis as it differs from electroless deposition, which usually requires a reducing agent. Adigun et al. investigated the underlying mechanisms of virus coating during the hydrothermal synthesis[14]. The adsorption models of TMV and TMV2Cys (TMV with the insertion of two additional cysteine groups) were described and fitted. It was concluded that the insertion of additional cysteine groups did not increase the adsorption capacity. Moreover, the total free chlorine content in the solution was

found to have an adverse effect on the mineralization process as it has a higher affinity to TMV than that of the metal ion precursor, thus, would limit the rate of mineralization. Subsequently, barley stripe mosaic virus (BSMV) was proposed as an alternative biotemplate. It is indicated that BSMV had much faster kinetics than TMV in terms of adsorption. However, the kinetics model considered $PdCl_3(H_2O)^-$ as the dominant species. The study did not consider the hydrolysis reaction of tetrachloropalladate(II) at low concentration. To the best of our knowledge, other palladium species resulted from the hydrolysis reaction of tetrachloropalladate(II) in aqueous solution would cause the formation of polynuclear Pd hydroxo complex clusters.

The hydrolysis of palladium(II) chloro complexes has been studied for several decades[15-16]. Perchloric acid is commonly used to suppress the hydrolysis reaction of tetrachloropalladate(II). However, the counterions in the system would affect the adsorption of Pd precursor ion, which is not applicable to the biotemplating synthesis. In addition, the acidic environment is detrimental to the biotemplates[17]. Therefore, it is crucial to investigate optimal conditions that can suppress hydrolysis reactions without damaging the biotemplates. On the other hand, surfactants such as trioctylphosphine[18-19] or polyvinylpyrrolidone[20] are commonly used as stabilizers in the synthesis of nanoparticles. While surfactants may be able to stabilize the precursor ions and as-synthesized nanoparticles, their effects on the adsorption system in biotemplating remain unclear. Therefore, the use of surfactants is not practical for biotemplating.

In this study, we investigated methods to minimize the formation of hydrolyzed chloropalladate species that ultimately tend to form clusters that are detrimental to the successful formation of uniform Pd-coated biotemplates. The equilibrium calculations outlined the distribution of hydrolyzed chloropalladate species and provided insights into the preparation of Na_2PdCl_4 stock solutions. Dynamic light scattering was used to monitor the aggregation of hydrolyzed palladium(II) species in Na_2PdCl_4 stock solutions. Raman spectroscopy was conducted to characterize the palladium hydrolyzed products in Na_2PdCl_4 stock solutions, and the particles derived from the mineralization process. Transmission electron microscope was used to image the palladium coated BSMV nanorods. The results reveal that the addition of dilute hydrochloric acid in Na_2PdCl_4 solution can limit the hydrolysis reaction of tetrachloropalladate(II) and minimize the formation of hydrolyzed palladium clusters during the mineralization.

Materials and methods

Purification of BSMV. BSMV purification was carried out following the published procedures[21] .

Preparation of Na_2PdCl_4 stock solution. Sodium tetrachloropalladate (99.8%, Sigma Aldrich) was mixed in deionized water or dilute HCl solution to prepare Na_2PdCl_4 stock solution at various concentrations. The Na_2PdCl_4 solution was filtered with a 0.22-um syringe filter and the filtrate was used as the precursor for virus coating.

Equilibrium species distribution and equilibrium pH calculations. The generic hydrolysis reaction is expressed as:

$$PdCl_n(OH)_{4-n}^{-2} + H_2O \leftrightarrow PdCl_{n-1}(OH)_{5-n}^{2-} + Cl^- + H^+; n = 1, 2, 3, 4$$

The equilibrium pH and the distribution of palladium chlorohydroxo species were estimated based on the equilibrium constants reported by Elding[16].

Hydrothermal synthesis. The hydrothermal synthesis was carried out in a 20-mL scintillation vial at 57 °C for 30 min. The virus was diluted and prepared in deionized water before the synthesis. The Na_2PdCl_4 solution was added into the biotemplate solution at room temperature.

Dynamic light scattering (DLS). Dynamic light scattering was performed by NanoBrook 90Plus PALS. The sample was transferred to a polystyrene cuvette before measurement. The effective size of the sample was monitored for 2 min in one measurement and typically 10 measurements were performed for one sample.

Transmission electron microscope (TEM) imaging. Samples were imaged in a 200 kV Tecnai T20 TEM by placing 3 μL of the suspension onto formvar/carbon coated copper grids and the grid was allowed to dry.

Raman spectroscopy. Raman spectra were acquired by a Thermo Scientific DXR2 Raman Microscope equipped with a 633-nm laser. A 50-μm pinhole aperture was used, and the laser power was set to 7.0 mW for liquid samples. The scan range was set to 50-3,500 cm^{-1} with a resolution of 5.3–8.8 cm^{-1}.

Results and discussion

Sodium tetrachloropalladate(II) in aqueous solution, with a series of hydrolysis reactions, forms four types of palladium(II) species. One of the species, $PdCl_2(H_2O)_2$ or $PdCl_2(OH)_2^{2-}$, is known to form insoluble precipitates due to olation[22]. These insoluble precipitates would limit the lifetime of Na_2PdCl_4 stock solution. Typically, a Na_2PdCl_4 stock solution is prepared before hydrothermal synthesis and should be used immediately to avoid the formation of insoluble precipitates. The insoluble particle forms rapidly when the solution is at low concentration (< 1mM). To visualize the formation of insoluble particles in Na_2PdCl_4 stock solutions, various Na_2PdCl_4 solutions were prepared in deionized water at concentrations ranging from 1 to 30 mM. Digital images of the Na_2PdCl_4 stock solutions are shown in Figure S1. The Na_2PdCl_4 stock solution at 1 mM turned turbid within 30 minutes and formed insoluble particles after 30 days. DLS was used to further monitor the size of insoluble particle or palladium polynuclear hydroxo complexes at different times. The DLS results are summarized in Table S1. For the aqueous Na_2PdCl_4 solution at 1 mM, the effective diameter of palladium(II) complexes increased from 270 nm to 374 nm during the measurement. The average size of the complexes was 750 nm after 1 day and increased to 1107 nm after 2 days, indicating rapid aggregation of the complexes. On the other hand, for the aqueous Na_2PdCl_4 solution at 30 mM, the effective diameter of palladium(II) complexes was around 17 nm (excluding the outliers). However, the effective size of the 30 mM Na_2PdCl_4 solution increased and began to fluctuate after 1 day, which could be attributed to the aggregation of palladium(II) complexes or the formation of palladium(II) polynuclear complexes. A similar trend was observed in the 5 mM Na_2PdCl_4 solution.

As the hydrolysis reaction proceeds, hydronium ions are released from the dissociated water molecule. To check the extent of the hydrolysis reaction, the pH of the solution was measured at various times from freshly prepared to about 150 days (Table S1). The pHs in all Na_2PdCl_4 solutions started to decrease after the preparation, indicating the hydrolysis of tetrachloropalladate ion was undergoing and releasing the hydronium ion and corresponding palladium(II) chlorohydroxo species.

The stability constants reported by Elding were programmed to calculate the distribution of palladium(II) chlorohydroxo species[16]. The distribution of palladium(II) chlorohydroxo species and equilibrium pH are shown in Figure 1a. According to the estimation, the distribution of palladium(II) chlorohydroxo species in deionized water is a function of initial concentration of Na_2PdCl_4 solution. It is noteworthy that the lower the initial Na_2PdCl_4 concentration is, the higher the hydroxyl group is associated with the palladium(II) species. The palladium species with high hydroxyl content tend to form palladium hydroxides (Figure S2) through olation process at the reaction temperature (57 °C) of the hydrothermal reaction. The hydrothermal reaction was carried out in the absence of biotemplate to verify the formation of particles from highly hydrolyzed palladium species. All the samples shown in Figure S2 were solutions containing various concentrations of Na_2PdCl_4 without biotemplate after heating to 57 °C. The detailed compositions of the samples are listed in Table S2. As can be seen in Figure S2, samples #1 and #2 contained brown particles, indicating the formation of palladium hydroxides as the Na_2PdCl_4 stock solutions had higher proportions of palladium(II) species associated with hydroxyl group. Notably, the brown particles also form when the BSMV is coated with palladium. Therefore, the formation of brown particle in the solution did not indicate the formation of palladium-coated biotemplate.

Hydrothermal synthesis of BSMV using aged Na_2PdCl_4 stock solution was performed to see if the hydrolyzed palladium species causes the formation of irregular palladium particles. The TEM image of palladium-coated BSMV(Pd-BSMV) produced from using the aged Na_2PdCl_4 solutions is shown in Figure 1b. The Pd-BSMV nanorods were attached or covered by irregular particles, which were aggregated palladium polynuclear hydroxo complex(PHC) clusters. Similarly, the PHC clusters can be seen in Figure 1c. The formation of PHC clusters can be attributed to the hydrolyzed palladium species in the aged Na_2PdCl_4 stock solutions. The hydrothermal synthesis of BSMV using aged or low concentration Na_2PdCl_4 solutions is depicted in Figure 1d. The aged or low concentration Na_2PdCl_4 stock solution may contain small proportions of hydrolyzed palladium(II) chlorohydroxo species, which subsequently formed palladium polynuclear hydroxo complex. The PHC in the Na_2PdCl_4 stock solution is then introduced to the biotemplate solution, causing the formation of PHC clusters attached to the Pd-BSMV during the hydrothermal synthesis.

To minimize the formation of palladium PHC in Na_2PdCl_4 stock solutions, dilute hydrochloric acid was used as the solvent to prepare Na_2PdCl_4 in HCl solution. To verify if the addition of HCl would reduce the formation of palladium PHC, the effective particle size of palladium(II) species of the Na_2PdCl_4 in HCl solution was monitored by DLS and plotted in Figure 2a. Initially, both solutions had negligible size upon preparation. However, the effective particle size dramatically increased after 1 day for the solution at pH 2.83, whereas for the solution at pH 1.47 the effective particle size remained below 10 nm, suggesting few palladium PHC clusters or insoluble particles formed around this pH. The hydrothermal reaction was performed in the absence of biotmeplate using the HCl-added Na_2PdCl_4 stock solutions to verify if fewer particles would form. As shown in Figure S2, samples #3 and #4 did not form appreciable particles. However, sample #3 turned turbid after the hydrothermal reaction, while sample #4 was relatively clear compared to sample #3. This is because the pH of the Na_2PdCl_4 stock solution used in sample #4 (pH 1.47) was lower than that in sample #3 (pH 2.83). The hydronium and chloride ions prevented the hydrolysis reaction in the Na_2PdCl_4 stock solution from forming more hydrolyzed palladium species. The distribution of palladium(II) chlorohydroxo species and equilibrium pH using 24 mM HCl solution as the solvent are shown

in Figure 2b. As can be seen in Figure 2b, $PdCl_3OH^{(2-)}$ species becomes the dominant species when the initial Na_2PdCl_4 concentration is higher than 40 mM. The species that tend to form insoluble particles are reduced with the introduction of dilute HCl solution to the Na_2PdCl_4 stock solution. The HCl-added Na_2PdCl_4 stock solutions were used to carry out the hydrothermal synthesis in the presence of biotemplate. The detailed conditions of hydrothermal synthesis using HCl-added Na_2PdCl_4 stock solutions are shown in Table S4. Figure 2c and 2d show the Pd-BSMV nanorods prepared from 30 mM Na_2PdCl_4 in 24 mM HCl solution. The Pd-BSMV had fewer PHC clusters, but the palladium coating was not as uniform as those Pd-BSMV nanorods shown in Figure 1c. This is because the added free chloride ions in the stock solution have higher affinity to the virus surface, occupying the active sites for the palladium species[14]. As a result, the reduction of Pd was limited by the excess chloride ions in the reacting solution. The reduction of Pd was significantly slow in the top two samples in Table S4 as the ratios of $[Cl^-_{free}]$ to [Pd] were 24 and 4.8, respectively. Therefore, no coated BSMV was observed in the samples with the given reaction time. Figure 3a and 3b show the Pd-BSMV nanorods prepared from 180 mM Na_2PdCl_4 in 24 mM HCl solution. It is evident that the Pd-BSMV nanorods contained fewer PHC clusters because the Na_2PdCl_4 stock solution had higher initial concentration of Na_2PdCl_4 plus the introduction of 24 mM HCl solution. Therefore, the hydrolysis reaction was inhibited. The hydrothermal synthesis of BSMV using HCl-added Na2PdCl4 solution is depicted in Figure 3c. When HCl is used as the solvent, the formation of $PdCl_2(OH)_2^{2-}$ due to the hydrolysis of tetrachloropalladate ion is limited by the chloride ions and hydronium ions. However, as the chloride concentration increases in the HCl-added Na2PdCl4 stock solution, it will compete with the adsorption of $PdCl_3(OH)^{(2-)}$[14], leading to uneven Pd coatings on the surface of BSMV.

The aggregation of hydrolyzed palladium species is sensitive to temperature. The hydrothermal reaction was carried out in a cuvette in the absence of biotemplate to monitor the particle growth using the DLS. The Na_2PdCl_4 stock solution was composed of 30 mM Na_2PdCl_4 in 10 mM HCl solution. The Na_2PdCl_4 solution was added to 2 mL of deionized water before measurement. Figure 4a shows the DLS results of 0.75 mM Na_2PdCl_4 in 0.25 mM HCl solution at various temperatures. At room temperature, while the sample at 25 °C did not show much aggregation in the first 10 minutes, the effective diameters were about 126 nm after 30 minutes and 220 nm after 60 minutes. The sample at 40 °C showed a similar trend with a larger particle size during the measurement. The particle sizes were around 178 nm after 30 minutes and 268 nm after 60 minutes. The sample at 57 °C, which is the temperature for the hydrothermal synthesis, showed an obvious increase in the first 10 minutes. The particle size after 30 minutes was about 400 nm, which was more than twice as large as the size of the other two samples. This implies that the elevated temperature would promote the self-aggregation of hydrolyzed Pd species.

To further verify the temperature effect on the aggregation of hydrolyzed Pd species, the biotemplate solution and Na_2PdCl_4 stock solution were preheated to 57 °C separately before mixing. Figure 4b shows the TEM image of Pd-BSMV nanorods prepared using the preheated solutions. A few hydrolyzed Pd species clumps can be seen because the preheated Na_2PdCl_4 stock solution contained aggregated hydrolyzed Pd species. Moreover, these aggregated hydrolyzed Pd clumps could not be utilized to form smooth Pd coatings on the surface of BSMV so that a small proportions of BSMV was partially coated or uncoated. Figure 4c shows the TEM image of Pd-BSMV nanorods when only the biotemplate solution was preheated to 57 °C, i.e., the Na_2PdCl_4 stock solution was at room temperature. As can be seen in Figure 4c, the Pd-BSMV nanorods were twisted and intertwined, indicating that the palladium species were

hydrolyzed and aggregated before the adsorption and reduction. This is because the volume of the biotemplate solution (ca. 2000 μL) was much higher than the volume of the Na2PdCl4 stock solution (ca. 50 μL) that was added into the biotemplate solution. Hence, the hydrolyzed palladium species were heated immediately and formed a large agglomerate upon mixing. On the other hand, when both the biotemplate solution and Na_2PdCl_4 stock solution were mixed at room temperature, the Pd-BSMV nanorods generated from this approach were more uniform (Figure 4d). Such experimental design would limit the aggregation of palladium species in the Na_2PdCl_4 stock solution and thus allow the precursor ion to adsorb onto the surface of biotemplate, leading to monodisperse palladium coatings on the BSMV.

Raman spectroscopy was performed to identify the predominant palladium species in the Na_2PdCl_4 stock solutions. Figure 5a shows the Raman spectra of sodium tetrachloropalladate(II) powder. The peaks at around 300 cm^{-1} and 270 cm^{-1} are attributed to tetrachloropalladate(II) species[23]. The peaks at the positions can be seen as the indicators to determine the predominant species in Na_2PdCl_4 stock solution. Figure 5b shows the Raman spectra of Na_2PdCl_4 stock solutions at various concentrations. The Na_2PdCl_4 stock solution of 180 mM displays the two characteristic peaks representing tetrachloropalladate species[23]. On the other hand, the other solutions show a broad peak around 450 cm^{-1}, which is likely representing other palladium chlorohydroxo species. Figure 5c shows the Raman spectra of the particles (the particle shown in Figure S2 sample #1) collected by reacting 0.75 mM Na_2PdCl_4 solution. At this concentration, the hydrolysis reaction of tetrachloropalladate(II) led to the formation of $PdCl_2(OH)_2^{2-}$, which then turned into palladium oxide. All of the peaks in Figure 5c matched the characteristic peaks of PdO[24].

Conclusion

In conclusion, this study has examined the stability constants of palladium(II) chloro complexes in aqueous media. The formation of palladium polynuclear hydroxo particle in Na_2PdCl_4 stock solution was mitigated by preparing the sodium chloropalladate stock solutions in dilute HCl solution. The DLS data confirmed that the addition of HCl in Na_2PdCl_4 stock solution increased the shelf life of the Na_2PdCl_4 stock solution. In addition, the palladium PHC clusters in Pd-BSMV nanorods produced from HCl-added Na_2PdCl_4 stock solution was minimized. The mineralization mechanisms without and with extra chloride ions were proposed.

The effect of preheating on the morphology of Pd-BSMV nanorods was evaluated and it was shown that the preheating facilitated the aggregation of palladium hydroxo species. The Raman spectra of Na_2PdCl_4 stock solutions suggested that tetrachloropalladate ion was the dominant species in the 180 mM Na_2PdCl_4 stock solution. The palladium particle collected from the hydrolyzed palladium species was verified to be palladium oxide, indicating the hydrolysis reaction fostered the formation of insoluble particles. Taken together, this study has shown that the addition of dilute HCl solution can stabilize the Na_2PdCl_4 stock solution and minimize the formation of palladium PHC clusters, leading to uniform palladium coatings on BSMV. Future work on the biotemplate will involve kinetics of mineralization with the presence of chloride ion, genetic engineering, and bimetallic metallization to produce composite nanowires.

Acknowledgments

The research was funded by the National Science Foundation under Grant No. CBET2028618. The research was also supported by the Robert B. and Virginia V. Covalt Professorship of Chemical Engineering, the Purdue Department of Botany & Plant Pathology, the Purdue Research Foundation (Fellowships #60000025 and #60000029), the USDA National Institute of Food and Agriculture (Hatch Multistate Project S1075) and startup funds from the Purdue Colleges of Agriculture and Engineering. Electron microscopy was performed with the help of Dr. Christopher J. Gilpin, Laurie Mueller, and Robert Seiler in the Purdue Life Science Microscopy Facility

References

1. Lim, J.-S.; Kim, S.-M.; Lee, S.-Y.; Stach, E. A.; Culver, J. N.; Harris, M. T., Biotemplated aqueous-phase palladium crystallization in the absence of external reducing agents. *Nano letters* **2010,** *10* (10), 3863-3867.
2. Sahoo, P. C.; Kim, K.; Lee, J. H.; Han, J.-I.; Oh, Y.-K., Biomimetically synthesized hierarchical TiO2-graphitic carbon as anodic catalysts for direct alkaline sulfide fuel cell. *ACS Sustainable Chemistry & Engineering* **2015,** *3* (8), 1764-1770.
3. Ijiro, K.; Mitomo, H., Metal nanoarchitecture fabrication using DNA as a biotemplate. *Polymer journal* **2017,** *49* (12), 815-824.
4. Ma, J.; Fan, H.; Ren, X.; Wang, C.; Tian, H.; Dong, G.; Wang, W., A simple absorbent cotton biotemplate to fabricate SnO2 porous microtubules and their gas-sensing properties for chlorine. *ACS Sustainable Chemistry & Engineering* **2018,** *7* (1), 147-155.
5. Cai, Q.; Liu, C.; Yin, C.; Huang, W.; Cui, L.; Shi, H.; Fang, X.; Zhang, L.; Kang, S.; Wang, Y., Biotemplating synthesis of graphitic carbon-coated TiO2 and its application as efficient visible-light-driven photocatalyst for Cr6+ remove. *ACS Sustainable Chemistry & Engineering* **2017,** *5* (5), 3938-3944.
6. Adigun, O. O.; Retzlaff-Roberts, E. L.; Novikova, G.; Wang, L.; Kim, B.-S.; Ilavsky, J.; Miller, J. T.; Loesch-Fries, L. S.; Harris, M. T., BSMV as a biotemplate for palladium nanomaterial synthesis. *Langmuir* **2017,** *33* (7), 1716-1724.
7. Hosseini, M.; Ahmadi, Z.; Khoobi, M.; Dehghani, S.; Kefayat, A., High-performance spirulina–bismuth biohybrids for enhanced computed tomography imaging. *ACS Sustainable Chemistry & Engineering* **2020,** *8* (34), 13085-13099.
8. Tseng, R. J.; Tsai, C.; Ma, L.; Ouyang, J.; Ozkan, C. S.; Yang, Y., Digital memory device based on tobacco mosaic virus conjugated with nanoparticles. *Nature nanotechnology* **2006,** *1* (1), 72-77.
9. Lee, K. Z.; Basnayake Pussepitiyalage, V.; Lee, Y. H.; Loesch-Fries, L. S.; Harris, M. T.; Hemmati, S.; Solomon, K. V., Engineering tobacco mosaic virus and its virus-like-particles for synthesis of biotemplated nanomaterials. *Biotechnol J* **2021,** *16* (4), 2000311.
10. Lee, S.-Y.; Royston, E.; Culver, J. N.; Harris, M. T., Improved metal cluster deposition on a genetically engineered tobacco mosaic virus template. *Nanotechnology* **2005,** *16* (7), S435.
11. Lee, S.-Y.; Choi, J.; Royston, E.; Janes, D. B.; Culver, J. N.; Harris, M. T., Deposition of platinum clusters on surface-modified tobacco mosaic virus. *Journal of nanoscience and nanotechnology* **2006,** *6* (4), 974-981.
12. Bromley, K. M.; Patil, A. J.; Perriman, A. W.; Stubbs, G.; Mann, S., Preparation of high quality nanowires by tobacco mosaic virus templating of gold nanoparticles. *Journal of Materials Chemistry* **2008,** *18* (40), 4796-4801.

13. Lim, J.-S.; Kim, S.-M.; Lee, S.-Y.; Stach, E. A.; Culver, J. N.; Harris, M. T., Quantitative study of Au (III) and Pd (II) ion biosorption on genetically engineered Tobacco mosaic virus. *Journal of colloid and interface science* **2010,** *342* (2), 455-461.
14. Adigun, O. O.; Novikova, G.; Retzlaff-Roberts, E. L.; Kim, B.; Miller, J. T.; Loesch-Fries, L. S.; Harris, M. T., Decoupling and elucidation of surface-driven processes during inorganic mineralization on virus templates. *Journal of colloid and interface science* **2016,** *483*, 165-176.
15. Srivastava, S. C.; Newman, L., Mixed ligand complexes of palladium (II) with chloride and bromide. *Inorganic Chemistry* **1966,** *5* (9), 1506-1510.
16. Elding, L. I., Palladium (II) halide complexes. I. Stabilities and spectra of palladium (II) chloro and bromo aqua complexes. *Inorganica Chimica Acta* **1972,** *6*, 647-651.
17. Lee, K. Z.; Pussepitiyalage, V. B.; Lee, Y. H.; Loesch-Fries, L. S.; Harris, M. T.; Hemmati, S.; Solomon, K. V., Engineering Tobacco Mosaic Virus and Its Virus-Like-Particles for Synthesis of Biotemplated Nanomaterials. *Biotechnol J* **2021,** *16* (4).
18. Son, S. U.; Jang, Y.; Yoon, K. Y.; Kang, E.; Hyeon, T., Facile synthesis of various phosphine-stabilized monodisperse palladium nanoparticles through the understanding of coordination chemistry of the nanoparticles. *Nano Lett* **2004,** *4* (6), 1147-1151.
19. Kim, S. W.; Park, J.; Jang, Y.; Chung, Y.; Hwang, S.; Hyeon, T.; Kim, Y. W., Synthesis of monodisperse palladium nanoparticles. *Nano Lett* **2003,** *3* (9), 1289-1291.
20. Sophia, J.; Muralidharan, G., Polyvinylpyrrolidone stabilized palladium nanospheres as simple and novel electrochemical sensor for amperometric hydrogen peroxide detection. *Journal of Electroanalytical Chemistry* **2015,** *739*, 115-121.
21. Namba, K.; Pattanayek, R.; Stubbs, G., Visualization of protein-nucleic acid interactions in a virus: Refined structure of intact tobacco mosaic virus at 2.9 Å resolution by X-ray fiber diffraction. *J Mol Biol* **1989,** *208* (2), 307-325.
22. Kettemann, F.; Wuithschick, M.; Caputo, G.; Kraehnert, R.; Pinna, N.; Rademann, K.; Polte, J., Reliable palladium nanoparticle syntheses in aqueous solution: the importance of understanding precursor chemistry and growth mechanism. *CrystEngComm* **2015,** *17* (8), 1865-1870.
23. Tait, C. D.; Janecky, D. R.; Rogers, P. S., Speciation of aqueous palladium (II) chloride solutions using optical spectroscopies. *Geochimica et Cosmochimica Acta* **1991,** *55* (5), 1253-1264.
24. Weber, W.; Baird, R.; Graham, G., Raman investigation of palladium oxide, rhodium sesquioxide and palladium rhodium dioxide. *Journal of Raman spectroscopy* **1988,** *19* (4), 239-244.

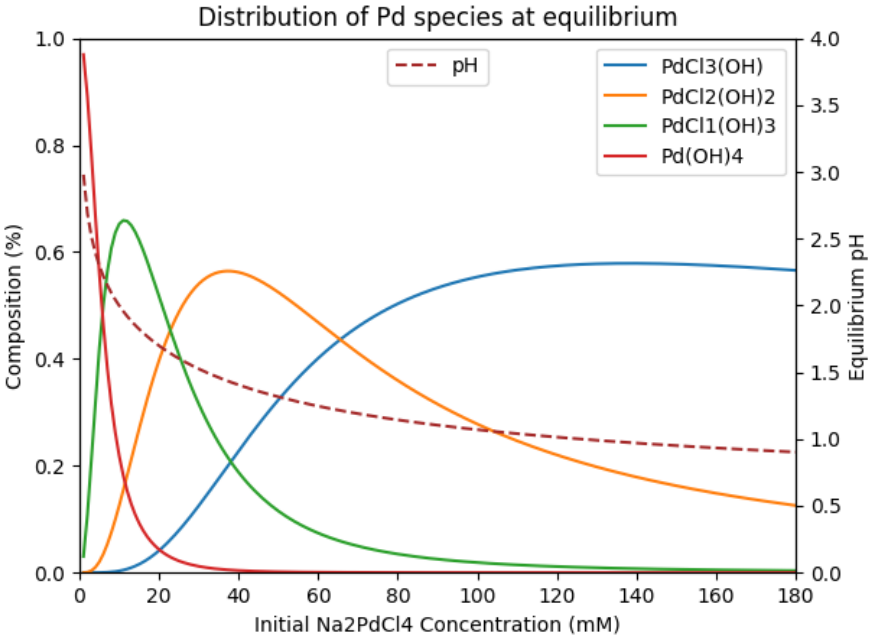

Figure 1a. The model predicted equilibrium pH and distribution of palladium(II) chlorohydroxo species in Na_2PdCl_4 stock solution at various initial concentrations (the stability constants were obtained from Elding).

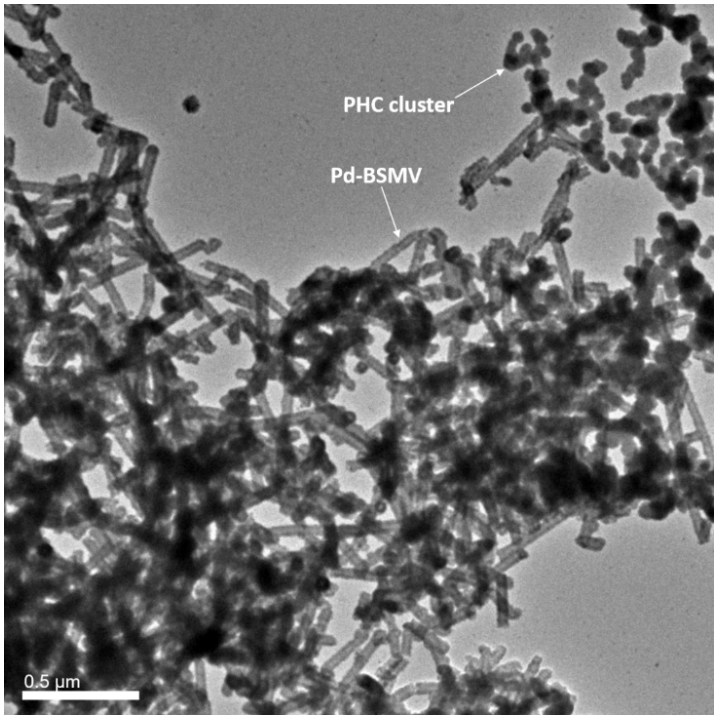

Figure 1b. Transmission electron microscopy image of palladium coated BSMV nanorods (3 coatings). The Pd-BSMV nanorods were collected after incubation of 0.035 mg/mL of BSMV in 0.75 mM of Na_2PdCl_4 (stock solution: 30 mM of Na_2PdCl_4 in deionized water, age: 2 days).

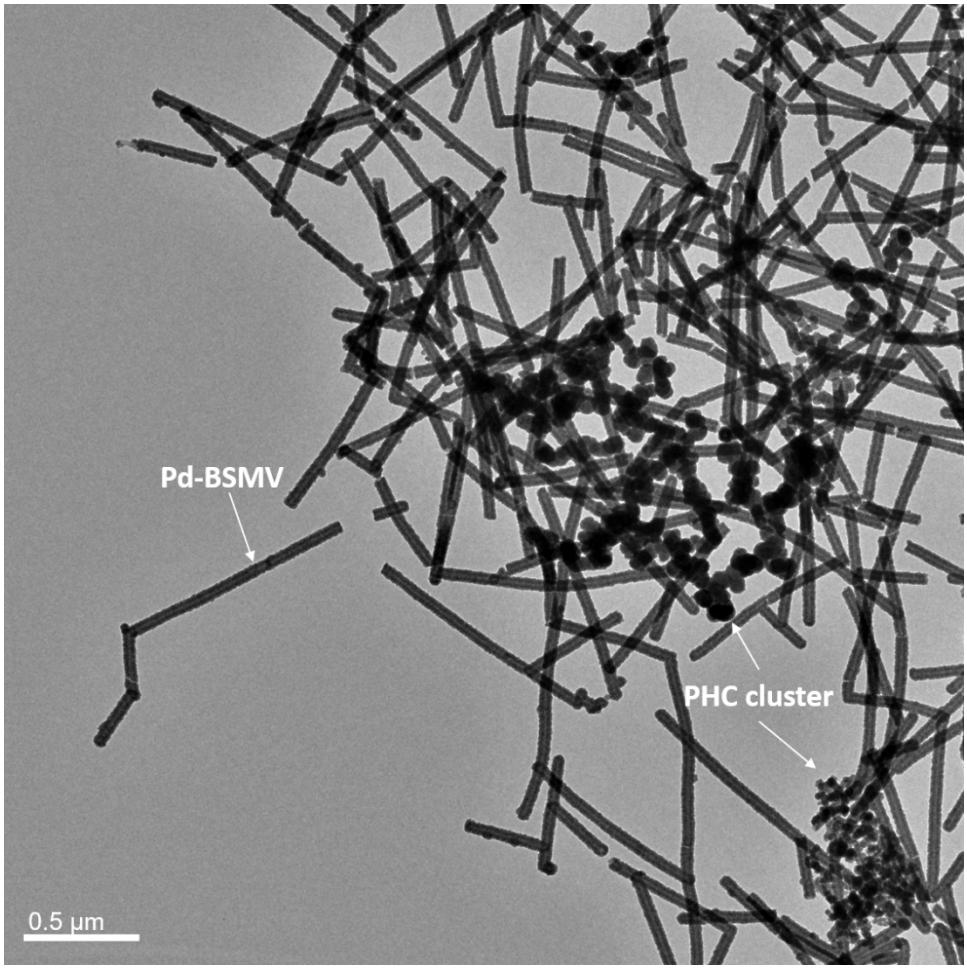

Figure 1c Transmission electron microscopy image of palladium coated BSMV nanorods (3 coatings). The Pd-BSMV nanorods were collected after incubation of 0.035 mg/mL of BSMV in 0.75 mM of Na_2PdCl_4 (stock solution: 180 mM of Na_2PdCl_4 in deionized water, age: 5 days).

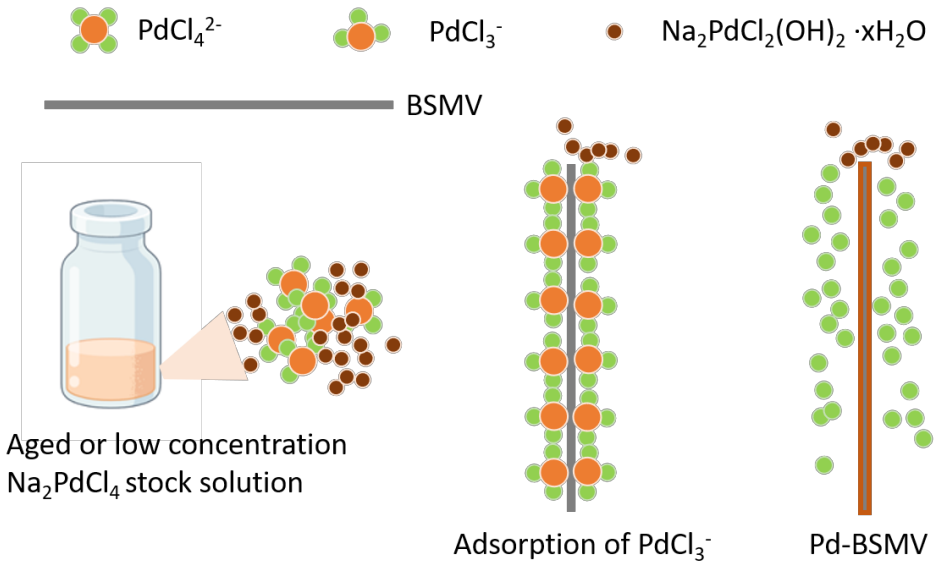

Figure 1d. Illustration of the hydrothermal synthesis of BSMV when an aged or low-concentration Na_2PdCl_4 stock solution is used as the palladium(II) precursor for coating.

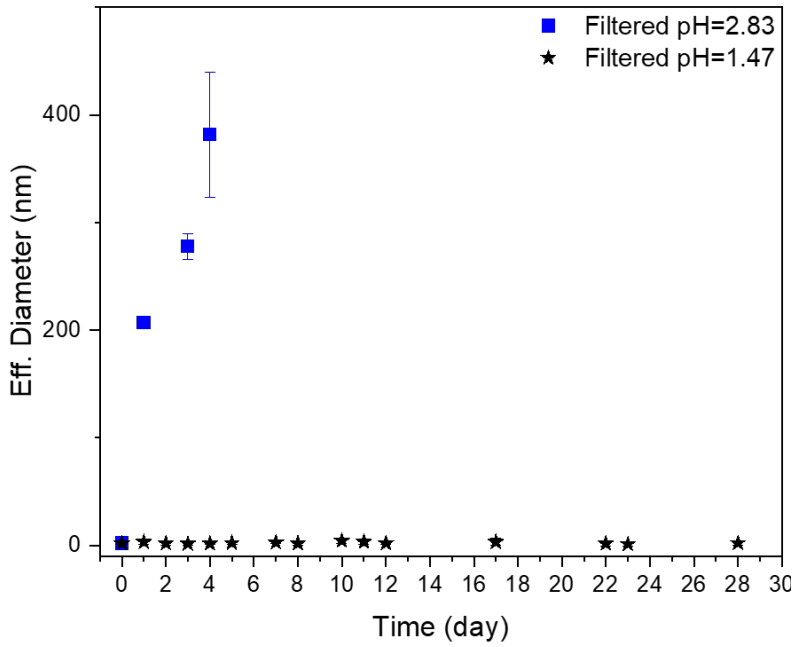

Figure 2a Dynamic light scattering measurements of 30 mM Na_2PdCl_4 in HCl solution.

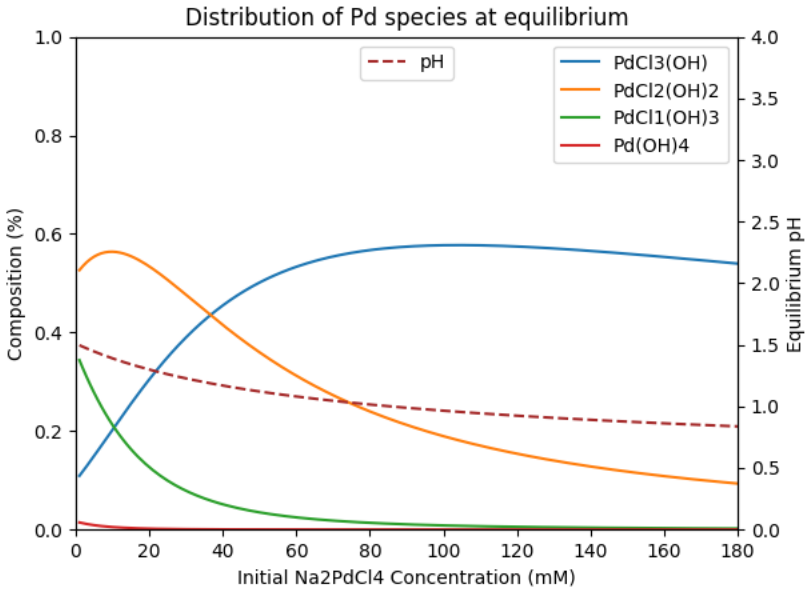

Figure 2b. The model predicted equilibrium pH and distribution of palladium(II) chlorohydroxo species in Na_2PdCl_4 stock solution at various concentrations (the stability constants were obtained from Elding). The system has an initial chloride concentration of 24 mM with a pH of 1.5.

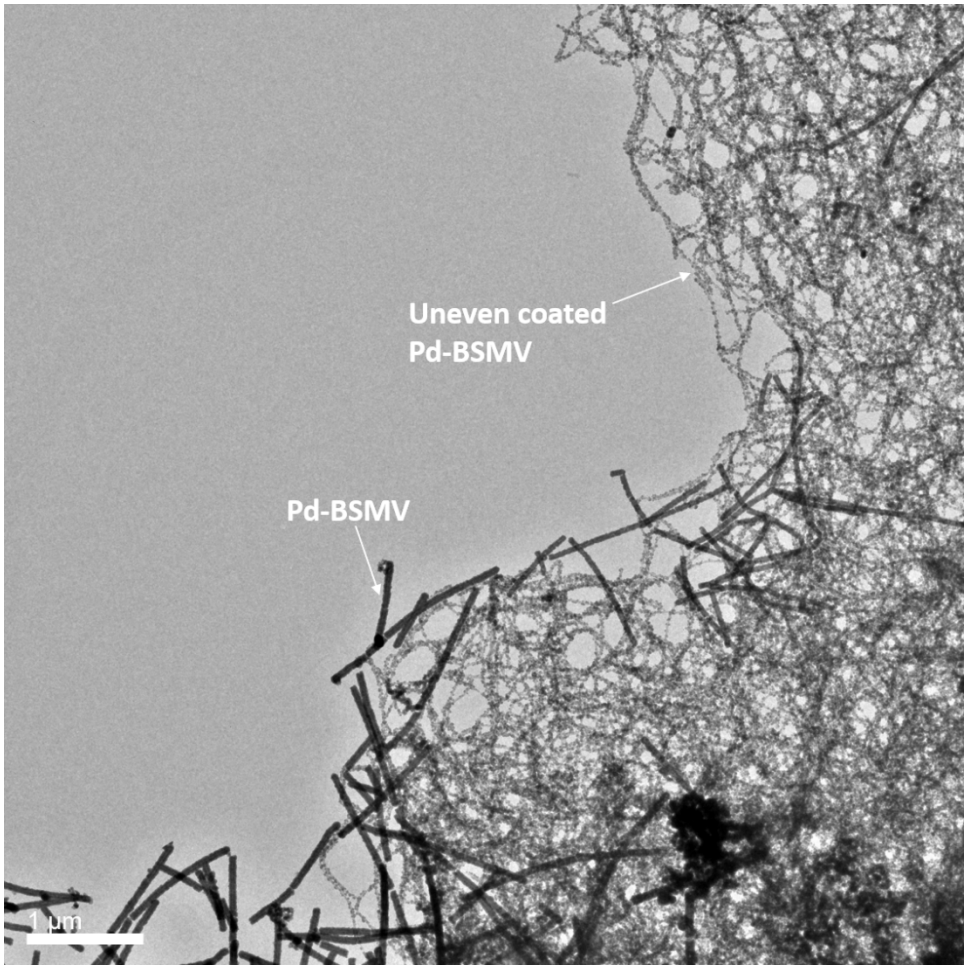

Figure 2c Transmission electron microscopy image (low magnitude) of palladium coated BSMV nanorods (3 coatings). The Pd-BSMV nanorods were collected after incubation of 0.035 mg/mL of BSMV in 0.61 mM of Na_2PdCl_4 (stock solution: 30 mM Na_2PdCl_4 in 24 mM HCl solution, fresh).

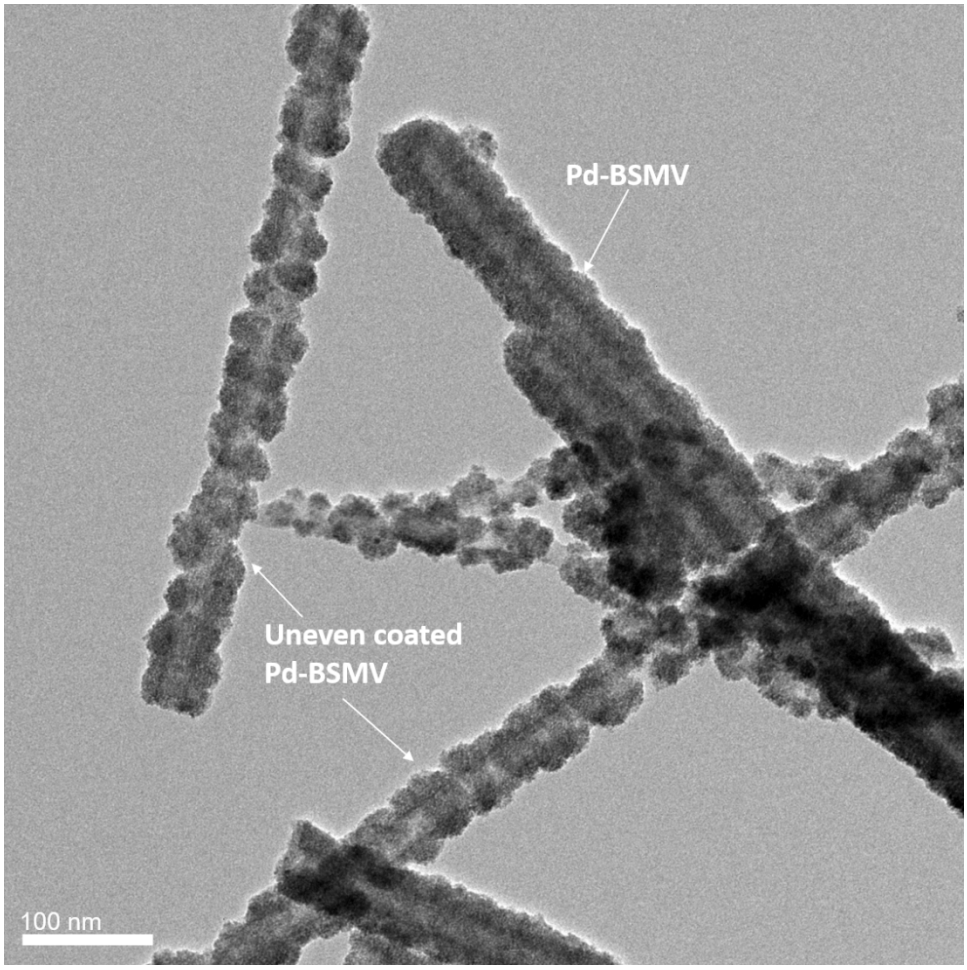

Figure 2d Transmission electron microscopy image (high magnitude) of palladium coated BSMV nanorods (3 coatings). The Pd-BSMV nanorods were collected after incubation of 0.035 mg/mL of BSMV in 0.61 mM of Na_2PdCl_4 (stock solution: 30 mM Na_2PdCl_4 in 24 mM HCl solution, fresh).

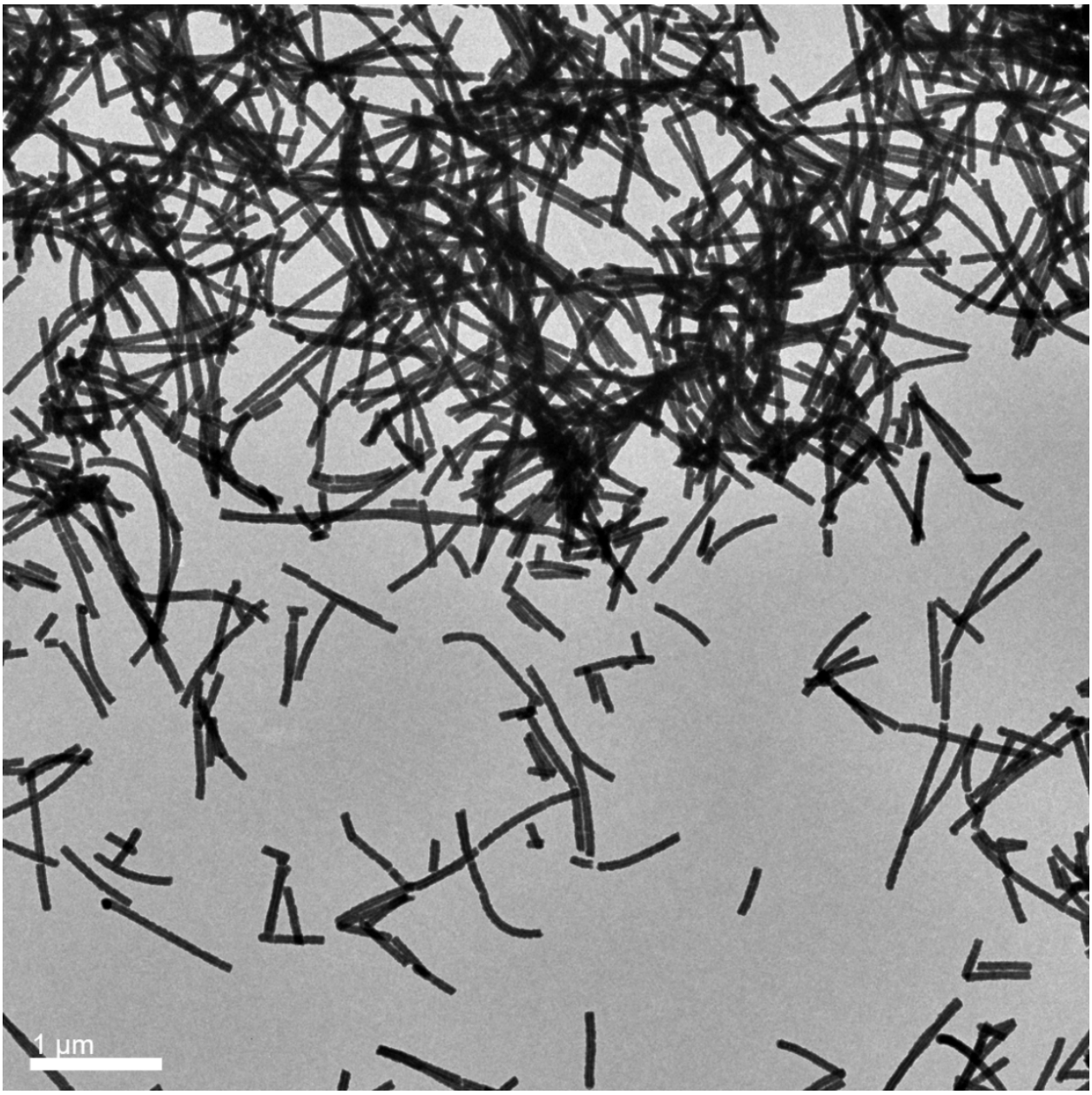

Figure 3a Transmission electron microscopy image (low magnitude) of palladium coated BSMV nanorods (3 coatings). The Pd-BSMV nanorods were collected after incubation of 0.035 mg/mL of BSMV in 0.75 mM of Na_2PdCl_4 (stock solution: 180 mM Na_2PdCl_4 in 24 mM HCl solution, fresh).

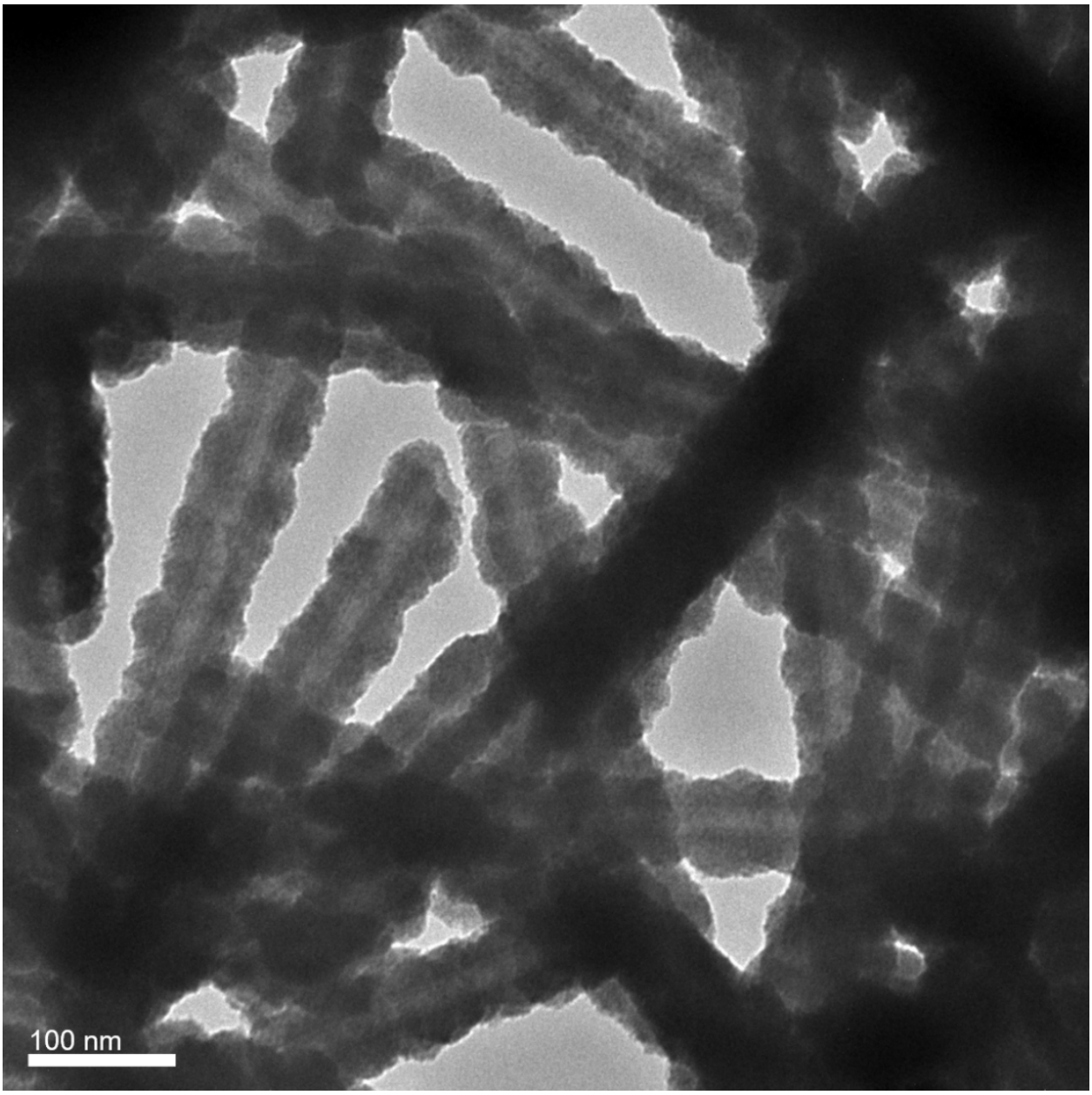

Figure 3b Transmission electron microscopy image (high magnitude) of palladium coated BSMV nanorods (3 coatings). The Pd-BSMV nanorods were collected after incubation of 0.035 mg/mL of BSMV in 0.75 mM of Na_2PdCl_4 (stock solution: 180 mM Na_2PdCl_4 in 24 mM HCl solution, fresh).

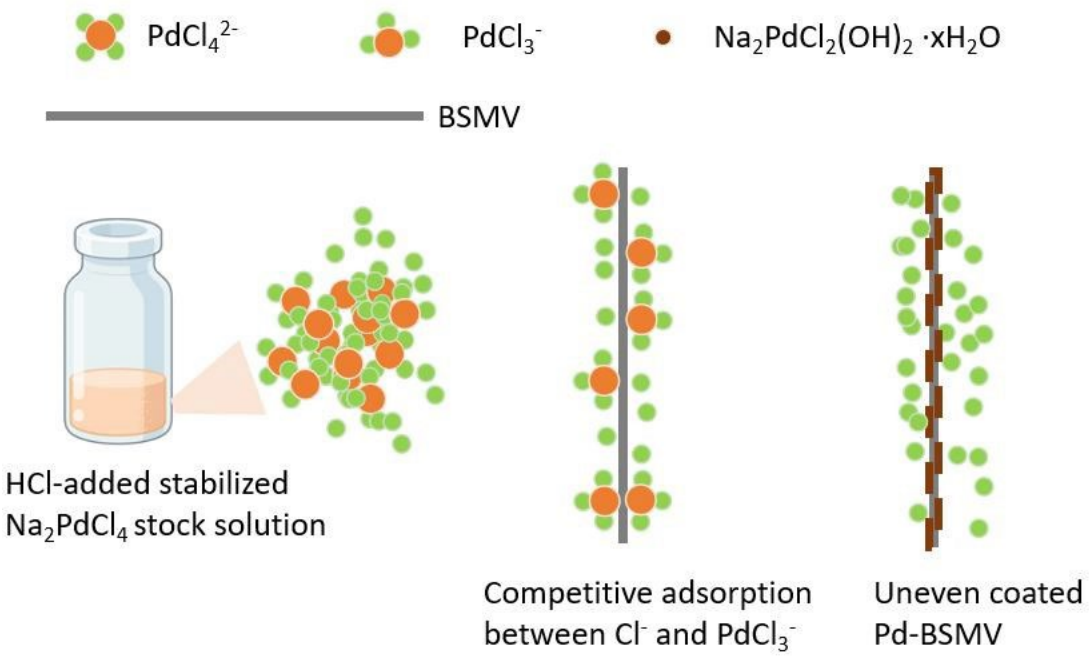

Figure 3c Illustration of the hydrothermal synthesis of BSMV when an HCl-added Na_2PdCl_4 stock solution is used as the palladium(II) precursor for coating.

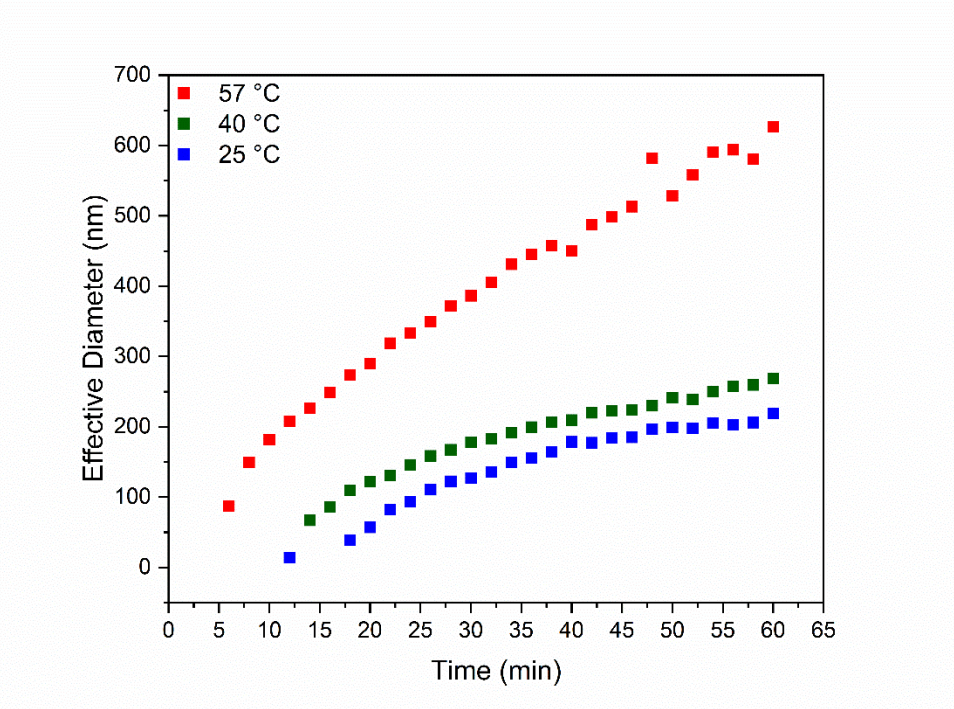

Figure 4a. Effective diameters of 0.75 mM Na_2PdCl_4 in 0.25 mM HCl solution at various temperatures.

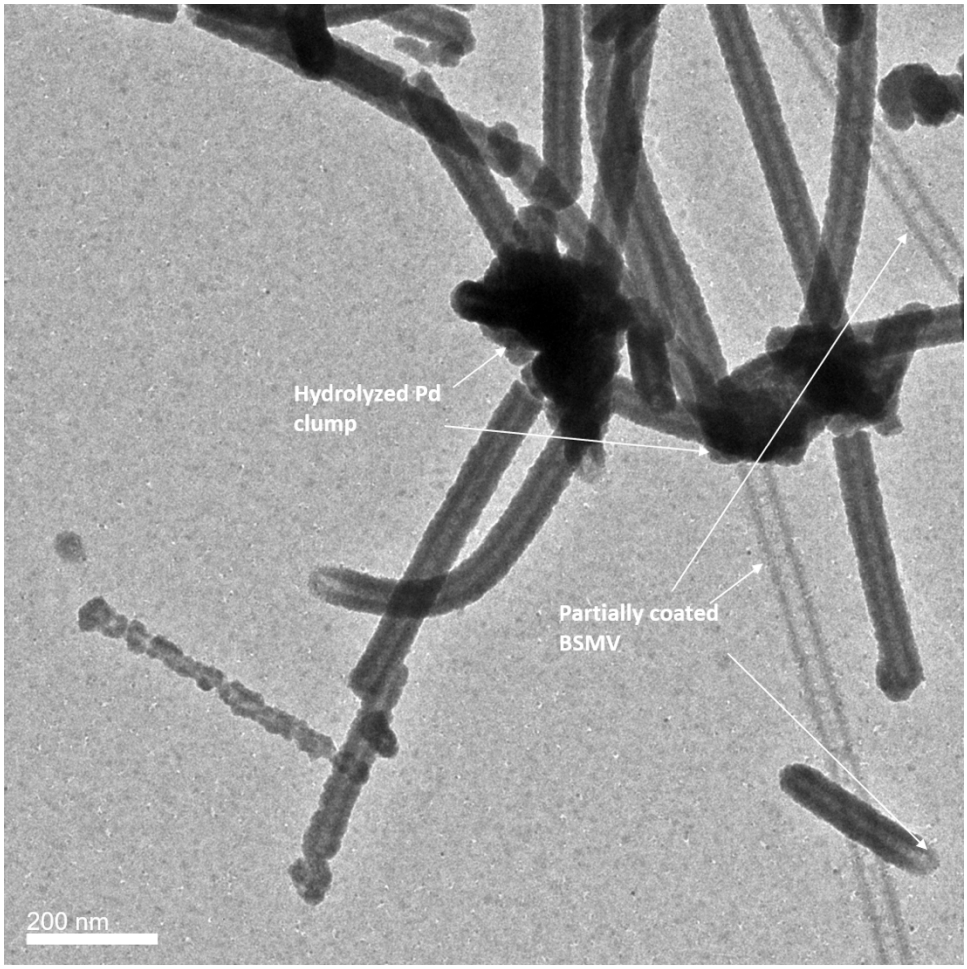

Figure 4b. Transmission electron microscopy image of palladium coated BSMV nanorods (2 coatings). The Pd-BSMV nanorods were collected after incubation of 0.035 mg/mL of BSMV in 0.75 mM of Na_2PdCl_4 (stock solution: 30 mM Na_2PdCl_4 in 10 mM HCl solution, fresh). The Na_2PdCl_4 and biotemplate solutions were preheated to 57 °C and, after mixing, the reacting solution was incubated for 30 min.

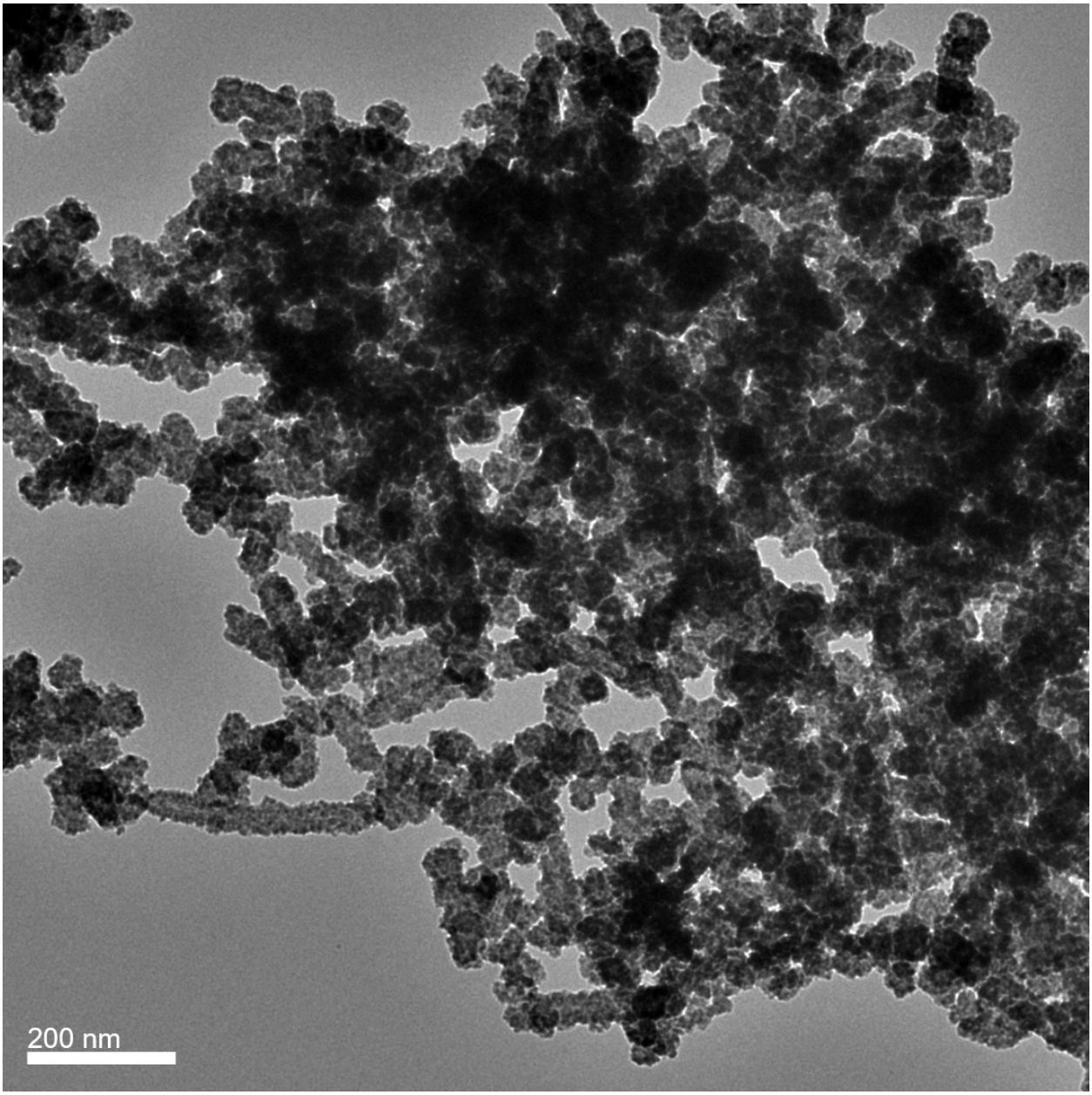

Figure 4c Transmission electron microscopy image of palladium coated BSMV nanorods (2 coatings). The Pd-BSMV nanorods were collected after incubation of 0.035 mg/mL of BSMV in 0.75 mM of Na_2PdCl_4 (stock solution: 30 mM Na_2PdCl_4 in 10 mM HCl solution, fresh). The biotemplate solution was preheated to 57 °C before the Na_2PdCl_4 solution was added and the reacting solution was incubated for 30 min.

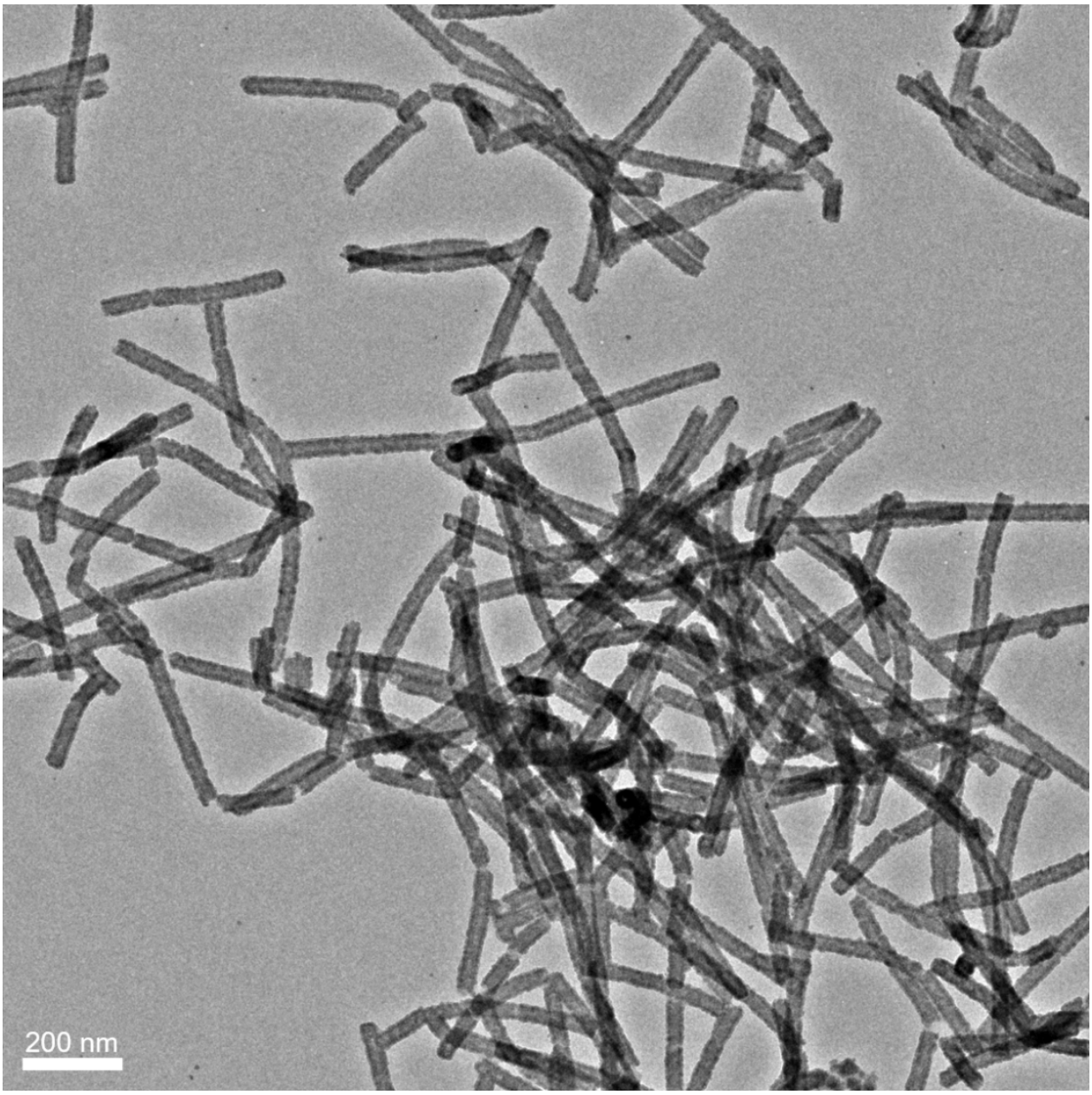

Figure 4d. Transmission electron microscopy image of palladium coated BSMV nanorods (2 coatings). The Pd-BSMV nanorods were collected after incubation of 0.035 mg/mL of BSMV in 0.75 mM of Na_2PdCl_4 (stock solution: 30 mM Na_2PdCl_4 in 10 mM HCl solution, fresh). The Na_2PdCl_4 and biotemplate solutions were mixed at room temperature and the reacting solution was then heated to 57 °C for 30 min.

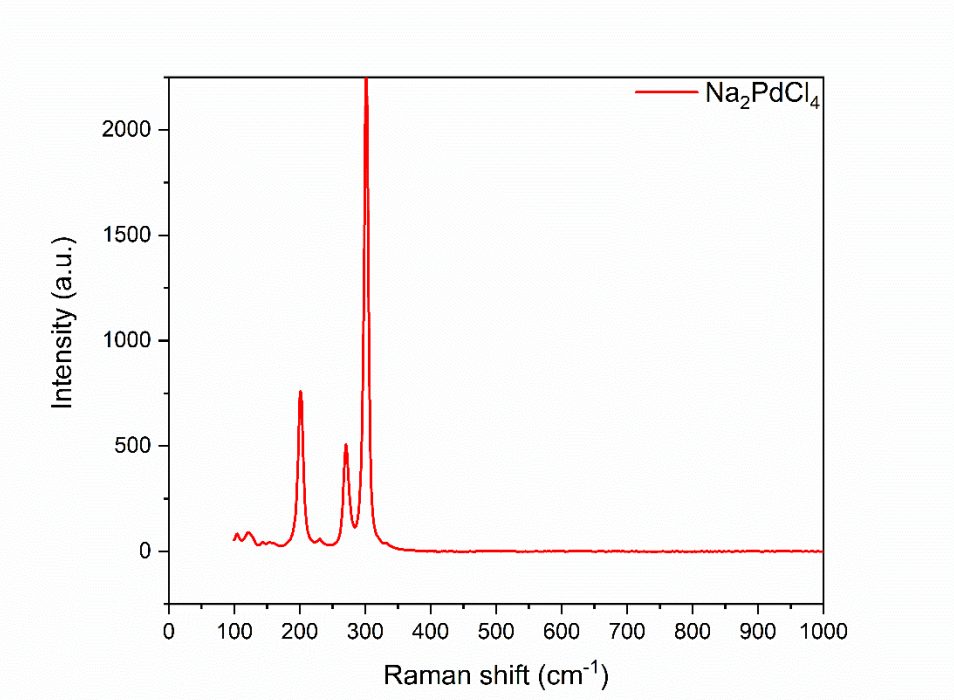

Figure 5a. Raman spectra of sodium tetrachloropalladate powder.

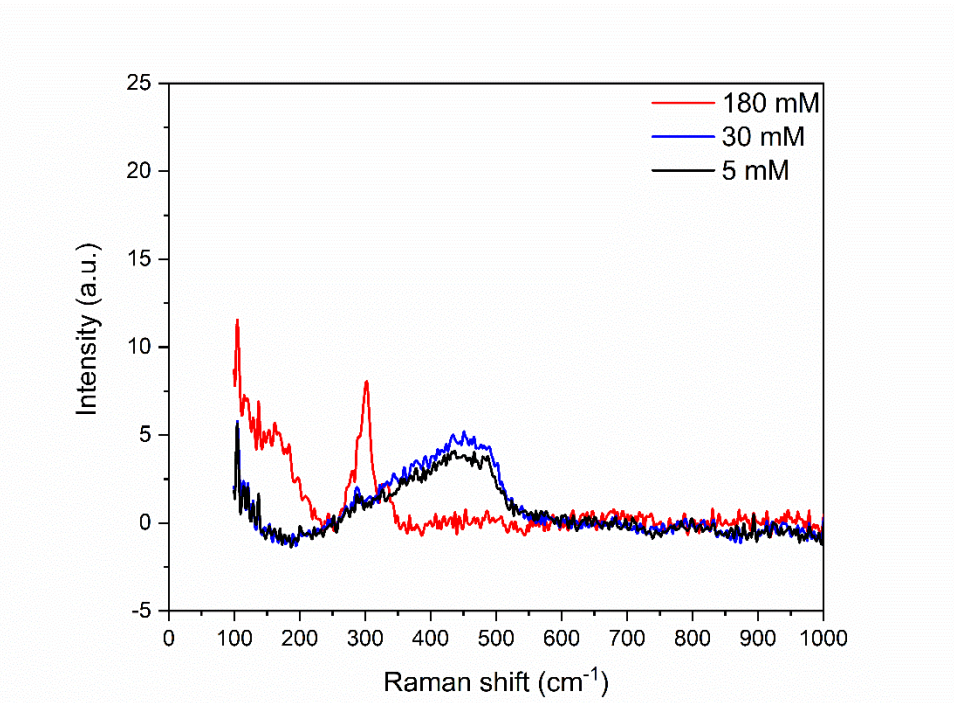

Figure 5b. Raman spectra of Na_2PdCl_4 stock solution at various concentrations.

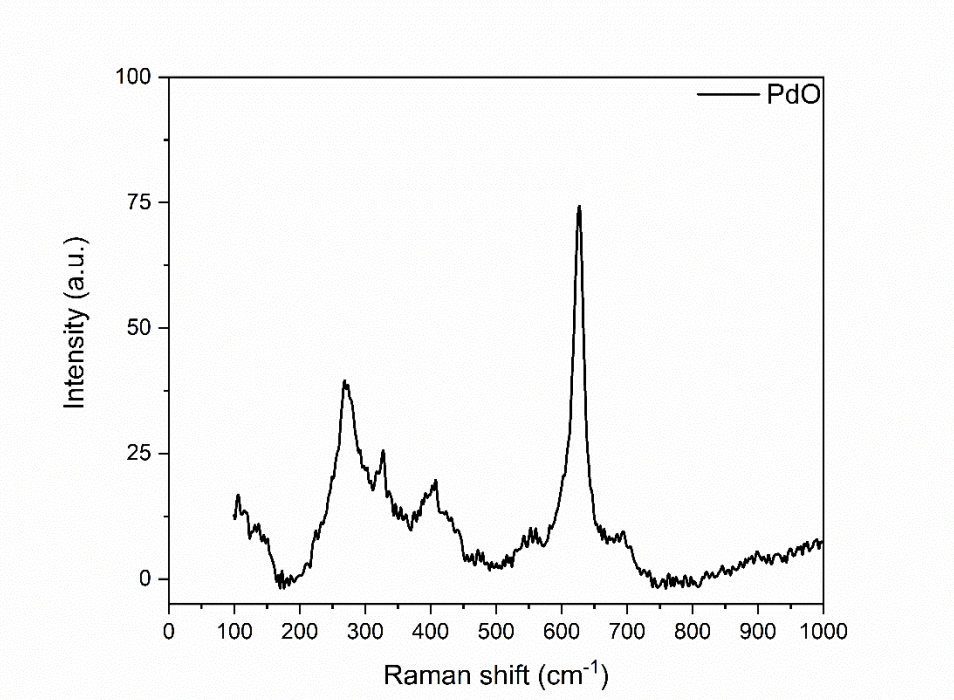

Figure 5c. Raman spectra of the particle collected from the incubation of 0.75 mM Na2PdCl4 solution at 57 °C for 30 minutes.